Dynamic Behaviour of Nanoscale Electrostatic Actuators *

LIN Wen-Hui(林文惠), ZHAO Ya-Pu(赵亚溥)**
State Key Laboratory of Nonlinear Mechanics, Institute of Mechanics, Chinese Academy of Sciences, Beijing 100080

(Received 9 July 2003)

The dynamic behaviour for nanoscale electrostatic actuators is studied. A two parameter mass-spring model is shown to exhibit a bifurcation from the case excluding an equilibrium point to the case including two equilibrium points as the geometrical dimensions of the device are altered. Stability analysis shows that one is a stable Hopf bifurcation point and the other is an unstable saddle point. In addition, we plot the diagram phases, which have periodic orbits around the Hopf point and a homoclinic orbit passing though the unstable saddle point.

PACS: 85. 85. +j, 02. 30. Oz

Nanoelectromechanical systems (NEMS), young sibling of microelectromechanical systems (MEMS), are an emerging field of research combining fundamental questions in physics with applications of nanotechnology.[1] Roughly speaking, NEMS are about 1000 times smaller than MEMS, as a matter of fact, the van der Waals (vdW) force and other surface forces, which can be neglected when designing MEM switches, play important roles in nanoscales.[2,3] NEM switches are fundamental building blocks for the design of NEMS applications, such as nanotweezers and some other nanoscale actuators.[4,5] Both MEM and NEM switches are often characterized by an inherent instability, as is known as pull-in phenomenon. The typical electrostatic actuators are built with two parallel conducting planes, where one is fixed and the other is movable. The two planes are supported by different styles such as fixed–fixed, cantilever and so on. In each case, a voltage difference between the two planes causes the upper movable conductor to deflect downward to the ground plane because of the electrostatic attraction. At a certain voltage, the movable conductor becomes unstable and spontaneously collapses (or *pulls in*) to the ground plane. Using one-dimensional (1D) model, Osterberg obtained the analytical expression of the pull-in parameters about MEM switches.[6] A lumped two-degree-of-freedom (L2DOF) pull-in model was presented in Ref. [7] for a direct calculation of the electrostatic actuators. The effect of residual charges, located in dielectric coating layers, upon the pull-in parameters of electrostatic actuators was studied.[8] The pull-in phenomenon is widely applied in many micromachined devices that require bi-stability for their operation, such as electrical rf switches[9] and some other micro-opto-electro-mechanical systems (MOEMS) devices.[10] Dequesnes *et al.* studied the pull-in voltage with the vdW force when neglecting the influence of the vdW force on the pull-in gap.[11] Rokin[12] considered the effect of the vdW force on the pull-in gap, and gave the analytical expression of the pull-in gap and pull-in voltages with a general model. The bifurcation analysis for an electrostatic microactuator has been addressed in Refs. [13,14] without the consideration of the vdW force. It was found that zero to two equilibrium points may exist, only one of which is stable. In this Letter, the bifurcation behaviour of the nanoscale electrostatic actuators considering the vdW force and its dynamics behaviour are discussed.

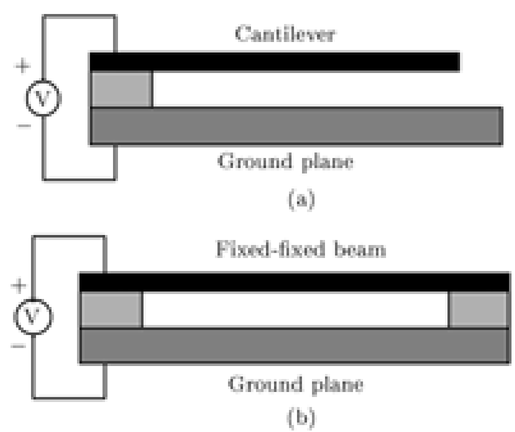

Fig. 1. Schematic of actuators: (a) cantilever and (b) fixed–fixed beam.

To simplify the analysis, the geometry model shown in Fig. 1 is usually substituted by a one-dimensional lumped model as shown in Fig. 2. The model consists of a linear spring, a mass, and a parallel-plane capacitor. Applying Newton's second law to this system, we obtain the second-order differential equation as follows

$$md^2u/dt^2 = F_{res} + F_{elec} + F_{vdW}, \quad (1)$$

* Supported by the Distinguished Young Scholar Fund of the National Natural Science Foundation of China under Grant No 10225209, the Key Project from the Chinese Academy of Sciences under Grant No KJCX2-SW-L2, and the National Key Basic Research Special Foundation of China under grant No G1999033103.

**To whom correspondence should be addressed.

where m is the mass of the plane. The electrostatic force acting between the planes with potential difference V is given by $F_{\rm elec} = \varepsilon_0 hLV^2/2(g-u)^2$, where g is the gap between the two planes, h is the width of the rectangle, L is the length of the beam, ε_0 is the permittivity of vacuum within the gap, and u is the deflection from its equilibrium position at $u = 0$. The vdW force resulting from the interaction between instantaneous dipole moments for atoms is given by $F_{\rm vdW} = AhL/6\pi(g-u)^3$, where $A = \pi^2 C\rho^2$ is the Hamaker constant which lies in the range (0.4–4)10^{-19}J, ρ is the volume density of graphite, and C is a constant character in the interactions between the two atoms. The restoring force of the plane is assumed to take the standard mass-spring form $F_{\rm res}(u) = -ku$, where k is the spring constant for the plane, the spring constant $k = 8EI/L^3$ for a cantilever structure, $k = 384EI/L^3$ for a fixed–fixed structure, E is Young's modulus, and $I = ht^3/12$ is the moment of inertia. Introducing five dimensionless variables, $w = (g-u)/g$, $\tau = t/T$, $M = m/kT^2$, $a = AhL/\pi kg^4$, $b = \varepsilon_0 hLV^2/kg^3$, we can transform the dynamic equation into

$$M{\rm d}^2w/{\rm d}\tau^2 = -b/2w^2 - a/6w^3 + (1-w). \qquad (2)$$

According to the definition of these parameters, physically relevant solutions exist in the region $0 < w < 1$. The parameter a denotes the ratio between the vdW and the restoring forces, b is the ratio between the electrostatic and the restoring forces, M is the ratio between the inertia and the restoring forces, and τ is the dimensionless time.

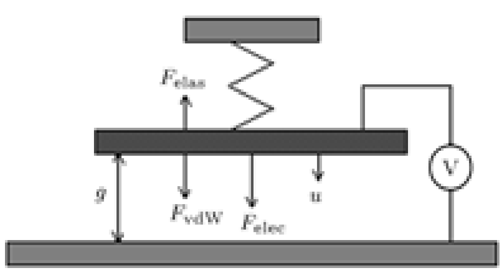

Fig. 2. One-dimensional lumped model for pull-in parameters estimation.

Set $\dot{w} = y$, Eq. (2) can be transformed into the following form

$$\frac{{\rm d}w}{{\rm d}\tau} = y,$$
$$M\frac{{\rm d}y}{{\rm d}\tau} = -\frac{b}{2w^2} - \frac{a}{6w^3} + (1-w). \qquad (3)$$

According to Eq. (3), the equilibrium points are

$$y = 0,$$
$$-\frac{b}{2w^2} - \frac{a}{6w^3} + (1-w) = 0.$$

At equilibrium points, the system is at rest. The second equation is equivalent to

$$f(w,a,b) = -3bw - a + 6w^3(1-w) = 0. \qquad (4)$$

This equation has two parameters a and b. We numerically solve Eq. (4) for as functions of a and b. The solution number is shown in Fig. 3. From this figure, we know that: no solution exists in $0 < w < 1$ when the value of a is larger than the critical values of $\tilde{a}^*$; less than $\tilde{a}^*$, two solutions exist in $0 < w < 1$ for any given $b_0 \geq 0$. The critical value of a can be determined by $f(w,a,b_0) = 0$ and $\partial f/\partial w(w,a,b_0) = 0$. If we set $b_0 = 0$, we can obtain the corresponding critical values of $a^* = 81/128$ and $w^* = 0.75$.

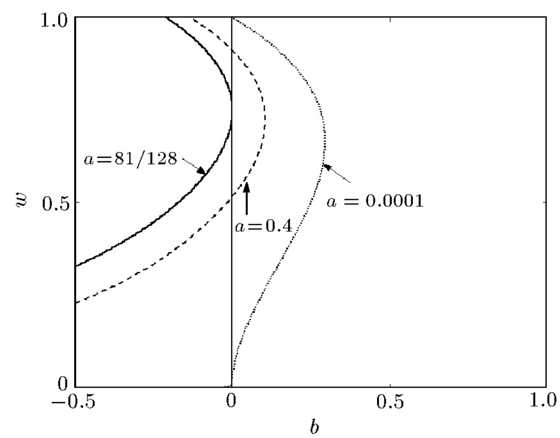

Fig. 3. Variation of equilibrium points with parameter b for different a values.

From the above discussion, we know that Eq. (3) has two equilibrium points with parameter a less than some critical value for any given b. The diagram is shown in Fig. 4.

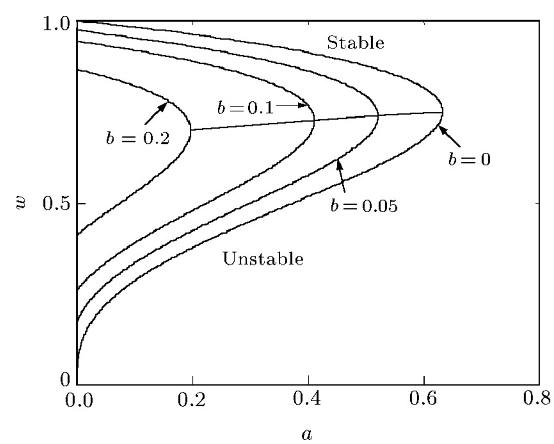

Fig. 4. Bifurcation diagram: variation of equilibrium points with parameter a for given different b.

In order to check for stability, we need the Jacobian matrix

$$\begin{bmatrix} 0 & 1 \\ \dfrac{b}{w^3}+\dfrac{a}{2w^4}-1 & 0 \end{bmatrix}.$$

We first discuss the stability of the equilibrium points with the given parameters $b = 0$ and $a_0 < a^*$. According to Fig. 4, there are two equilibrium points $(w_1, 0)$ and $(w_2, 0)$ satisfying the inequality $w_1 > w^* > w_2$.

Substituting the equilibrium point $(w_1, 0)$ into the Jacobian matrix, we can know that its corresponding eigenvalue satisfies $\lambda^2 = a_0/2w_1^4 - 1 < 0$. It has two pure imaginary roots, which means that the equilibrium point $(w_1, 0)$ is a stable Hopf bifurcation point. Applying the same method for the other equilibrium point $(w_2, 0)$, we know that it is an unstable saddle point. Then we can plot the phase diagram as shown in Fig. 5. There exist periodic orbits around a Hopf bifurcation point, and there is a homoclinic orbit passing through the saddle point.

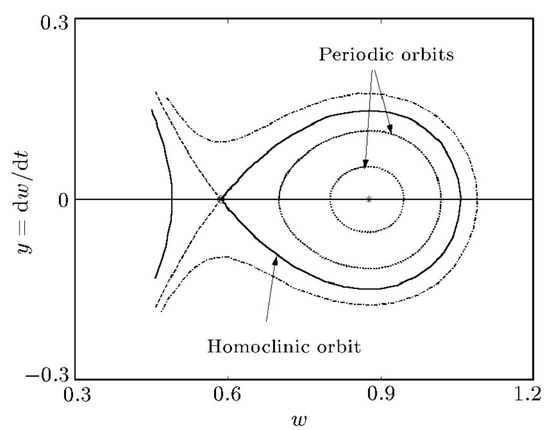

Fig. 5. Phase diagram with given $a = 1/2$ and $b = 0$.

With the same method, we discuss the stability of the two solutions with any different given a and b, and plot its corresponding phase diagram. These results are plotted in Figs. 4 and 6.

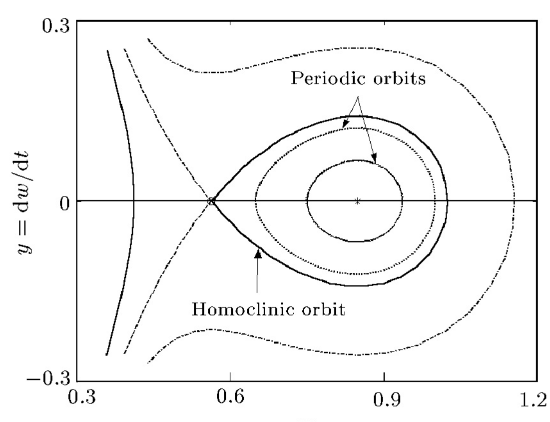

Fig. 6. Phase diagram with given $a = 0.3$ and $b = 0.1$.

The detachment length is the maximum length for cantilever or fixed–fixed plane that will not adhere with the substrate due to the vdW force. It is interesting to note that the detachment length of the cantilever and fixed–fixed plane can be obtained by the critical value $a^* = 81/128$. That is, the detachment length of the cantilever that will not adhere with the substrate due to the vdW force is

$$L_{\max} = \frac{\sqrt{6}}{4} g \sqrt[4]{\frac{3\pi E t^3}{A}}, \tag{5}$$

and the detachment length of the fixed–fixed is

$$L'_{\max} = \frac{3\sqrt{2}}{2} g \sqrt[4]{\frac{\pi E t^3}{A}}. \tag{6}$$

From Fig. 7, we could see the variation of the minimum gap with length of the cantilever and fixed–fixed switches, respectively.

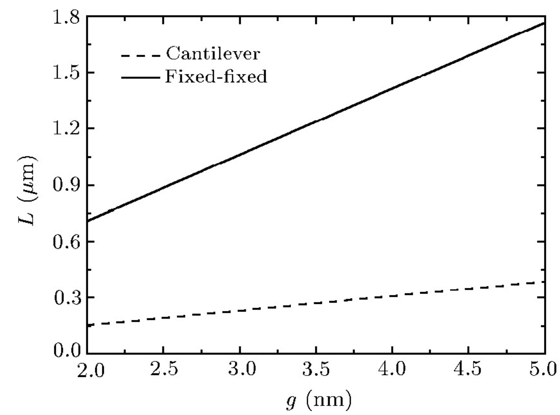

Fig. 7. Variation of the detachment length with the initial gap.

As an alternative case, if the length is known, we can calculate the minimum gap. The detachment lengths of the cantilever and fixed–fixed beam have been determined by critical value $a^* = 81/128$, which are fundamental design parameters for NEM actuators.

In conclusion, we have presented a theoretical analysis of dynamics behaviour of nanoscale electrostatic actuators. Using a simple mass-spring model we show that there exists bifurcation from the case excluding an equilibrium point to the case including two equilibrium points as the geometry of the device is altered. From Fig. 3, no solution exists in $0 < w < 1$ to satisfy $b \geq 0$ when the value of a is larger than the critical values $a^* = 81/128$. From the expression of the critical value a^*, we can obtain the detachment length $L_{\max} = \sqrt{6} g \sqrt[4]{3\pi E t^3/A}/4$ for cantilever plane, and $L'_{\max} = 3\sqrt{2} g \sqrt[4]{\pi E t^3 A}/2$ for fixed–fixed plane. This means that the movable plane will collapse onto the ground plane without any voltage difference when the length of plane is longer than the detachment length. The pull-in voltage is increasing with the ratio a being less seen from Figs. 3 and 4. Compared these results with Refs. [13,14], the vdW force will not change the number of equilibrium points and their corresponding stability. The attractive ability of the vdW force just decreases the pull-in voltage.

References

[1] Sapmaz S, Blanter Y M, Gurevich L and van der Zant H S J 2003 *Phys. Rev.* B **67** 235414

[2] Zhao Y P, Wang L S and Yu T X 2003 *J. Adhesion Sci. Technol.* **17** 519

[3] Zhao Y P and Li W J 2002 *Chin. Phys. Lett.* **19** 1161

[4] Kim P and Lieber C M 1999 *Science* **286** 2148

[5] Akita S et al 1991 *Appl. Phys. Lett.* **79** 1691

[6] Osterberg P M 1995 *PhD Dissertation* MIT, Cambridge, MA

[7] Bochobza-Degani O and Nemirovsky Y 2002 *Sensors and Actuators* A **97-98** 569

[8] Bochobza-Degani O, Socher E and Nemirovsky Y 2002 *Sensors and Actuators* A **97–98** 563

[9] Zhang L X and Zhao Y P 2003 *Microsyst. Technol.* **9** 420

[10] Hornbeck L J 1991 *US Patent* 5061049

[11] Dequesnes M, Rotkin S V and Aluru N R 2002 *Nanotechnol.* **13** 120

[12] Rotkin S V 2002 *Electrochem. Society Proc.* **6** 90

[13] Pelesko J A 2001 *Proc. Modelling and Simulation of Microsystems Conf.* (MSM 2001) 290

[14] Bernstein D, Guidotti P, Pelesko J A 2000 *Proc. Modelling and Simulation of Microsystems Conf.* (MSM 2000) 489